of the density distribution in the planet. ($C/MR^2 \simeq 0.33$ for the Earth, $\simeq 0.40$ for the Moon, $\simeq 0.40$ for an homogeneous sphere.)

Finally, measurement of the amplitude of the physical libration φ_0 yields $(B-A)/C_m$ from which three known factors yield

$$\left(\frac{C_m}{B-A}\right)\left(\frac{B-A}{MR^2}\right)\left(\frac{MR^2}{C}\right) = \frac{C_m}{C} \leq 1 \qquad (4)$$

A value for C_m/C of 1 would indicate the core to be firmly coupled to the mantle and hence most probably solid. If the entire core or the outer part is fluid, $C_m/C \simeq 0.5$ for the large core size ($R_c \simeq 0.75R$) in current models of the interior[5].

How good are the assumptions that a fluid core will not follow the short period physical librations but will follow the long period precession? The appropriate time scale to compare with the 88-d and 250,000-yr periods is the 'spin up' or 'spin down' time for the core fluid (rotating at a slightly different angular velocity) to approach the perturbed angular velocity of the mantle[11].

$$\tau = R_c/(\nu\dot{\psi})^{\frac{1}{2}} \qquad (5)$$

where R_c is the core radius, ν is the kinematic viscosity and $\dot{\psi}$ is the spin angular velocity of the planet. If $\tau > 88$ d the core will not follow the mantle libration, whereas if $\tau < 250{,}000$ yr, the core will follow the mantle precession. These bounds on τ lead to the bounds on ν of

$$8\times10^{-4} < \nu < 2\times10^{9}\ \text{cm}^2\ \text{s}^{-1} \qquad (6)$$

where both necessary conditions for the determination of C_m/C are satisfied if ν is within these bounds. This is almost certainly true since the range in equation (6) includes the complete range estimated for the Earth's core of 5×10^{-3}–10^7 cm² s⁻¹ (ref. 12).

The numbers φ_0, θ, J_2 and C_{22} must be determined to find C_m/C and hence the extent of the Mercurian liquid core. The first two are O(20″–40″) and O($\lesssim 1°$) (ref. 9, and B. A. Smith, personal communication) respectively and will almost certainly require rather sophisticated instrumentation on the surface of the planet. The latter two can be obtained from precise tracking of artificial satellites. The design of instrumentation to measure the small angles φ and θ which is within the weight limitations and which will survive the possibly hard landing of any spacecraft sent to Mercury's surface is a severe challenge. The large scientific return which could, however, be realised from such surface instrumentation means that the attempt at the design should be made.

S. J. PEALE

Department of Physics,
University of California,
Santa Barbara, California 93106

Received March 4; accepted July 7, 1976.

[1] Ness, N. F., Behannon, K. W., Lepping, R. P., Whang, Y. C., and Schatten, K. H., *Science*, **185**, 151–160 (1974).
[2] Ness, N. F., Behannon, K. W., Lepping, R. P., and Whang, Y. C., *J. geophys. Res.*, **80**, 2708–2716 (1975).
[3] Siegfried, R. W., II, and Solomon, S. C., *Icarus*, **23**, 192–205 (1974).
[4] Fricker, P. E., Reynolds, R. T., Summers, A. L., and Cassen, P. M., *Nature*, **259**, 293–294 (1976).
[5] Cassen, P. M., Young, R. E., Schubert, G., and Reynolds, R. T., *Icarus* (in the press).
[6] Peale, S. J., *Icarus* (in the press).
[7] Peale, S. J., *Icarus*, **17**, 168–173 (1972).
[8] Peale, S. J., *Astr. J.*, **79**, 722–744 (1974).
[9] Peale, S. J., *Astr. J.*, **74**, 483–489 (1969).
[10] Kaula, W. M., *EOS, Trans. Am. geophys. Un.*, **56**, 309–316 (1975).
[11] Greenspan, H. P., and Howard, L. N., *J. Fluid Mech.*, **17**, 385–404 (1963).
[12] Jeffreys, H., *The Earth*, 254 (Cambridge University Press, 1959).

Structure of the extended solar magnetic field and the sunspot cycle variation in cosmic ray intensity

THE interplanetary magnetic field within several astronomical units of the Sun appears to have one polarity in most of the hemisphere north of the solar equatorial plane and the opposite polarity in most of the hemisphere south of the equatorial plane[1–7]. The two hemispheres are separated by a curved current sheet that typically crosses the solar equatorial plane in either two or four places, thus dividing the equatorial region into either two or four sectors. Near sunspot minimum, at 1 AU the curved current sheet has a spread in latitude of typically ± 15°, so that the sector boundary (the current sheet separating the two hemispheres of opposed field polarity) is almost parallel to the solar equatorial plane. In the photosphere, on the other hand, the sector boundary makes an angle of ~ 90° with the equatorial plane[8]. At $1.5R_\odot$, in 1972 and 1973, the angle between the sector boundary and the equatorial plane was ~ 45° (ref. 9), and at 3–$10R_\odot$ the angle between boundary and plane was ~25° (ref. 10). A schematic diagram of this structure for the case of four sectors is shown in Fig. 1. We here propose that a connection exists between the extent of these magnetic fields and the observed variations in cosmic ray intensity at the Earth.

In the photosphere, near sunspot minimum, the sector magnetic fields cover a range in latitude of typically ±40° (ref. 8), while at 1 AU the comparable range in latitude has been compressed to perhaps ±15°. How is this compression in latitude accomplished? A typical magnitude of the sector magnetic fields in the photosphere is 0.5 gauss (P. H. Scherrer and T. L. Duvall, personal communication). This is a measure of the large scale field that will dominate in the region a few $R_\odot$ above the photosphere, where the smaller scale but much stronger fields associated with active regions do not reach. In the polar regions of the Sun the large scale unidirected photospheric field has a typical magnitude of perhaps 5 gauss (R. Howard, personal communication). Thus, at 1 or $2R_\odot$

Fig. 1 Schematic showing the warped current sheet in the inner Solar System (inside 6 AU). This current sheet divides the interplanetary magnetic field in the heliosphere into two regions with oppositely directed field lines. In one region the field polarity is away from the Sun (at present this region is north of the solar equator), in the other region the field polarity is toward the Sun. The situation is shown for a four-sector structure, that is, as the current sheet is rotated past a stationary observer in the course of a solar rotation, the observer will see four changes of magnetic polarity, suggesting that the interplanetary magnetic field is divided into four sectors of alternating polarity. Where the current sheet lies above the solar equatorial plane it is shown by full lines, while dashed lines indicate that the current sheet is below the equatorial plane. The extent in latitude of the current sheet was assumed to be ±15°. The Sun at the centre is not shown to scale.

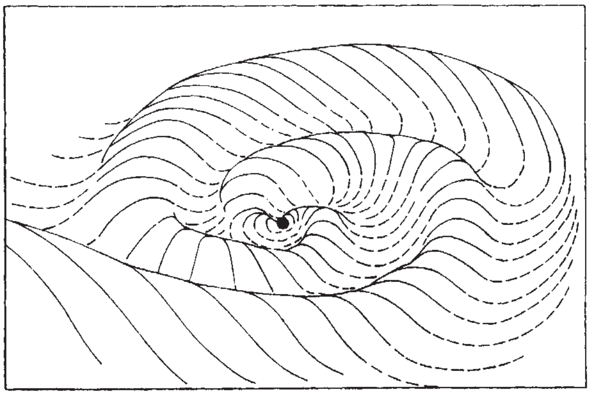

above the photosphere, and above the region of influence of active regions, the magnetic pressure associated with the solar polar regions is two orders of magnitude larger than the magnetic pressure associated with the equatorial sector structure. This will compress the equatorial sector field structure into a narrow range of latitudes. This effect can be clearly seen in the sketch in Fig. 2 made from an eclipse photograph taken at solar minimum in 1954 (ref. 11).

During an interval near sunspot maximum, when the solar polar field polarities are reversing, the magnitude of the polar fields may be considerably less, and the resulting compression of the equatorial field structure also much less. The sector structure fields may then occupy a much larger fraction of the heliosphere. Since the sector structure fields reverse polarity typically four times or two times per solar rotation, a galactic cosmic ray headed towards the Sun may encounter considerably more magnetic scattering from the complex sector structure field than from the unidirectional field that fills most of each solar hemisphere near sunspot minimum. This geometrical effect may be the principal cause of the 11-yr modulation of cosmic-ray intensity observed at the Earth, since the solar-wind velocity[12] and the magnitude of the interplanetary field[13] observed near the Earth have not changed very much during the present sunspot cycle.

The fraction of the heliosphere occupied by sector-structure fields as a function of time through an average sunspot cycle can be estimated in the following way. Because the current sheet shown in Fig. 1 is warped with respect to the solar equatorial plane, during the half year when the earth is north of the equatorial plane an interplanetary sector with the same polarity as the northern solar polar region is observed to be wider than it would be if observed when the Earth is in the equatorial plane of the Sun. For example, assume that there are two sectors per solar rotation and that the extent in heliographic latitude of the sector structure near the Earth is ±20°. When the Earth is at a latitude near 7°N (near September 7), the sector whose polarity is the same as the northern polar region will be observed to last 16.5 d, as compared with the 13.5 d it would last if observed when the Earth is near the solar equatorial plane. For comparison, if the extent in heliographic latitude of the sector structure near the Earth is ±45°, then the sector with the same polarity as the northern polar region will have a length of 14.6 d when observed near the Earth at 7°N. We see that if we measure the magnitude of this Rosenberg–Coleman effect[14,15] through a sunspot cycle we can estimate the extent in heliographic latitude of the sector structure.

We have used an harmonic analysis to compute the average amplitude of the Rosenberg–Coleman effect as a function of years from the time of sunspot minimum for the four sunspot cycles whose minima were near 1934, 1944, 1954 and 1965. Interplanetary field polarities inferred from polar geomagnetic variations[16] were used, and the resulting amplitude of the Rosenberg–Coleman effect was multiplied by 1.43 to correct for the ~85% accuracy[17,18] of the inferred interplanetary field polarities.

Figure 3 shows the resulting value for the extent in heliographic latitude of the sector structure through an average sunspot cycle. Three-year running means were used to reduce the scatter. Year 0 is the average of the sunspot minimum years 1934, 1944, 1954 and 1965. The effect of uncertainties in the computation of the magnitude of the Rosenberg–Coleman effect will usually be to decrease the amplitude of the effect and, therefore, the latitude values shown in Fig. 3 should be considered upper limits. We may expect considerable variation from the average effect shown in Fig. 3, and in particular for intervals of several months near sunspot minimum the current sheet may occupy only a few degrees of latitude.

As a first approximation, we assume that galactic cosmic rays have relatively difficult access to the inner Solar System in the portion of the heliosphere occupied by the changing fields of the sector structure, and relatively easy access through the portions of the heliosphere occupied by the extended uniform solar polar fields. This assumption is consistent with the observational evidence now available. A final evaluation must await *in situ* observations with out-of-ecliptic spacecraft. It is also observed[8] that high speed solar wind streams are contained within sectors. Kinks and irregularities in the interplanetary magnetic field that can scatter cosmic rays are produced as the fast plasma in a high speed stream overtakes slower plasma. The solar-wind plasma coming from higher solar latitudes may have a more uniform (albeit larger) velocity than the solar wind plasma from lower solar latitudes, and thus be not as effective in producing scattering of cosmic rays.

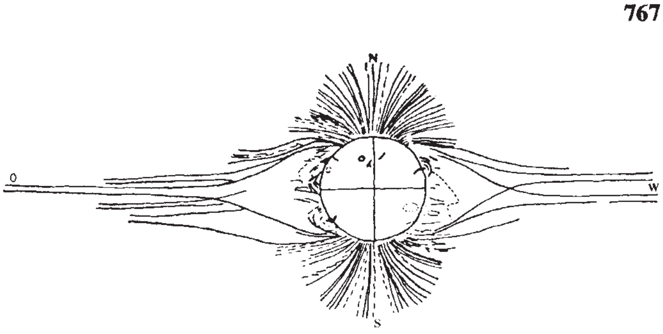

Fig. 2 The structure of a sunspot minimum solar corona drawn from eclipse photographs[11] (June 30, 1954) obtained in Kozeletsk.

In Fig. 4 we show the solid angle of the heliosphere occupied by the extended solar polar fields through an average sunspot cycle, where the latitude angles shown in Fig. 3 are used to compute the solid angles shown in Fig. 4. Also shown in Fig. 4 are the monthly averages of the absolute intensity of primary cosmic rays of rigidity > 0.5 GV observed near Murmansk and at Mirny from 1958 to 1973 (ref. 19). The total flux of such galactic cosmic rays in the interstellar medium in the vicinity of the earth is estimated to be 4,000 $m^{-2}\,s^{-1}\,sr^{-1}$ (ref. 19). Therefore, in Fig. 4 we have set the total solid angle 4π of the heliosphere as equivalent to a flux of 4,000 $m^{-2}\,s^{-1}\,sr^{-1}$, and the zero of the solid angle scale corresponds to zero flux. This corresponds to the assumption that galactic cosmic rays have easy access to the inner Solar System through the solid angle of the heliosphere occupied by the extended solar polar fields, and difficult access through the solid angle occupied by the sector structure fields.

In Fig. 4 we see that the average sunspot cycle variation of the solid angle of the extended solar polar fields is rather similar to the observed variation of the flux of primary cosmic rays of rigidity > 0.5 GV between 1961 and 1969. We should not

Fig. 3 Computed variation of the average extent in heliographic latitude of the extended solar sector magnetic fields. Year 0 is the average of the sunspot minimum years 1934, 1944, 1954 and 1965. The value 20° on the ordinate means that the extended sector fields are in the interval 20°N to 20°S.

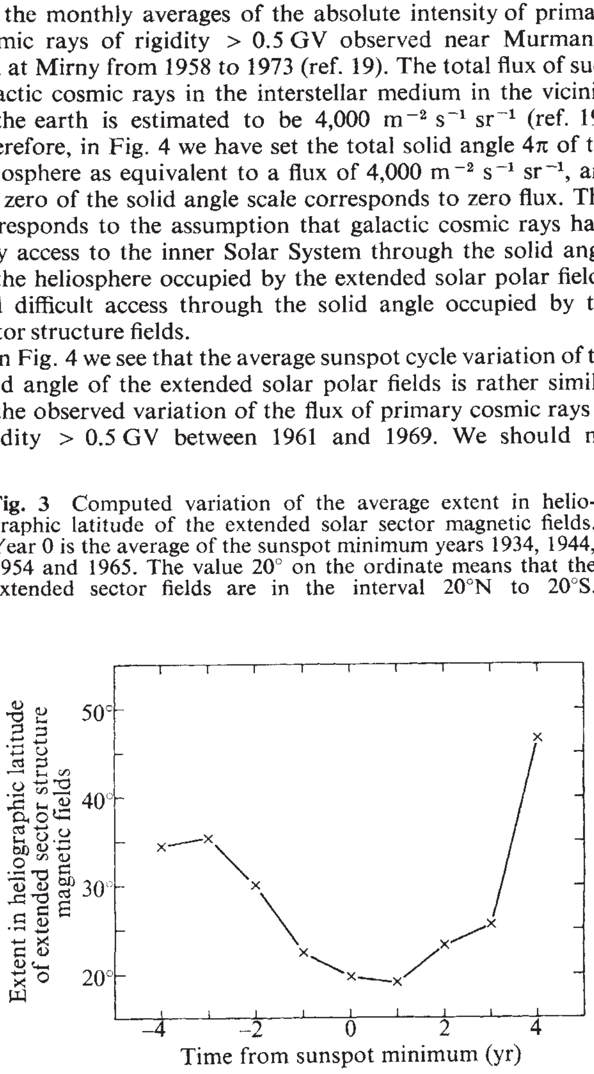

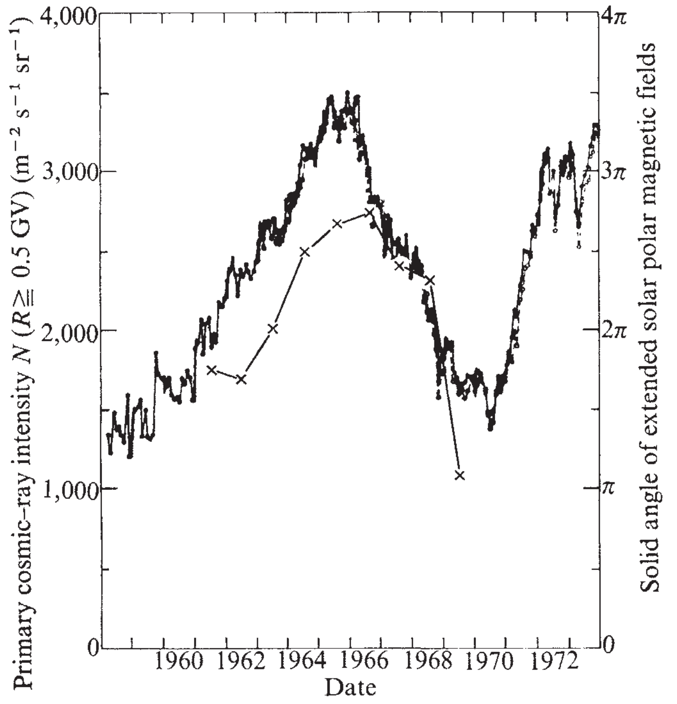

Fig. 4 Galactic cosmic-ray intensities with rigidity 0.5 GV observed near Murmask (●) and at Mirny (○) from 1958 to 1973 (ref. 19). Also shown is the computed average solid angle (×) of the heliosphere occupied by the extended solar polar magnetic fields.

expect a detailed agreement between the computed variation of solid angle averaged over four sunspot cycles and the observed cosmic-ray flux around a single sunspot minimum. The similarity of the two curves in Fig. 4 suggests that there may be some validity to the considerations advanced in this paper. The detailed computation of the diffusion lengths of cosmic rays related to these considerations is beyond the scope of this paper.

We thank the NASA-Skylab Workshop on Coronal Holes for discussions. This work was supported in part by the Office of Naval Research, by NASA, by the Atmospheric Sciences Section of the NSF and by the Max C. Fleischmann Foundation.

LEIF SVALGAARD
JOHN M. WILCOX

Institute for Plasma Research,
Stanford University,
Stanford, California 94305

Received March 22; accepted July 5, 1976.

[1] Schatten, K., *Solar Wind* (edit. by Sonnett, C. P., Coleman, P. J., and Wilcox, J. M.), 65–92 (Scientific and Technical Office, NASA, 1972).
[2] Schultz, M., *Astrophys. Space Sci.*, **24**, 371–383 (1973).
[3] Sawyer, C., *Geophys. Res. Lett.*, **1**, 295–297 (1974).
[4] Alfven, H., *Proc. Nobel Symposium on the Physics of Hot Plasma in the Magnetosphere* (Kiruna, Sweden, 1975).
[5] Levy, E. H., *Proc. 14th int. Cosmic Ray Conf., 15–29 August 1975*, **4**, 1215–1220 (Max-Planck-Institut für Extraterrestrische Physik, München, FRG, 1975).
[6] Svalgaard, L., Wilcox, J. M., Scherrer, P. H., and Howard, R., *Sol. Phys.*, **45**, 83–91 (1975).
[7] Saito, T., *Sci. Rep. Tohoku Univ., Geophys.*, **23**, 37–54 (1975).
[8] Wilcox, J. M., *Space Sci. Rev.*, **8**, 258–328 (1968).
[9] Hansen, S., Sawyer, C., and Hansen, R. T., *Geophys. Res. Lett.*, **1**, 13–15 (1974).
[10] Howard, R. A., and Koomen, M. J., *Sol. Phys.*, **37**, 469–475 (1974).
[11] Vsekhsvjatsky, S. K., *The Solar Corona, Proc. int. astr. Un. Symp., 16, Cloudcroft, New Mexico, 28–30 August 1961* (edit. by Evans, J. W.) 271–280 (Academic, New York, 1963).
[12] Diodato, L., Moreno, G., Signorini, C., and Ogilvie, K. W., *J. geophys. Res.*, **79**, 5095–5108 (1974).
[13] Barouch, E., and King, J. H., *Proc. 14th int. Cosmic Ray Conf., 15–29 August 1975*, **3**, 1036–1041 (Max-Planck-Institut für Extraterrestrische Physik, München, FRG, 1975).
[14] Rosenberg, R. L., and Coleman, P. J., Jr, *J. geophys. Res.*, **74**, 5611–5622 (1969).
[15] Wilcox, J. M., and Scherrer, P. H., *J. geophys. Res.*, 77, 5385–5388 (1972).
[16] Svalgaard, L., *J. geophys. Res.*, 77, 4027–4034 (1972).
[17] Russell, C. T., and Rosenberg, R. L., *Sol. Phys.*, **37**, 251–256 (1974).
[18] Wilcox, J. M., Svalgaard, L., and Hedgecock, P. C., *J. geophys. Res.*, **80**, 3685–3688 (1975).
[19] Vernov, S. O., Charakhchyan, A. N., Stozhkov, Ju. I., and Charakhchyan, T. N., *Proc. 14th int. Cosmic Ray Conf., 15–29 August 1975*, 3, 1015–1024 (Max-Planck-Institut für Extraterrestrische Physik, München, FRG, 1975).

Glass-rich basaltic sand and gravel within the oceanic crust at 22°N

DURING Leg 46 of the Deep Sea Drilling Project (January 29–March 10, 1976), the second leg of the International Phase of Oceanic Drilling, the Glomar Challenger drilled into 255 m of basaltic basement at hole 396B, 160-km east of the Mid-Atlantic Ridge valley at 22°59.14′N, 43°30.90′W. The hole was drilled into crust with a magnetic anomaly age of ~ 10 Myr. This site is located in a N–S trending sediment pond which measures ~ 4 km × 10 km and is concordant with local topographic trends. There are 150 m of sediment at the drill site; however, the basement slopes regionally to the east and sediment thickness is probably > 250 m along the fault-bounded (?) eastern margin (G. M. Purdy, unpublished, and report of work by the Soviet research vessel Akademik Kurchatov). The bottom 90 m of this hole contained basaltic sand and gravel. This material is not believed to be a drilling artefact, but caused by *in situ* spalling or brecciation of basaltic pillow rinds.

On a number of other occasions, for example, on Legs 34 and 45, there was some indication, principally the sticking or jamming of the drill bit within young basement, that clastic zones had been encountered. At hole 396B a zone of rapid penetration was followed by an interval of difficult drilling and frequent sticking of the bit which eventually led to termination of drilling. In the lower part of the hole, the core catcher assembly was modified to catch fine clastic material and in cores 30 and 33, the core barrel contained 82 and 90 cm respectively, of basaltic gravel and sand. The recovery rate immediately above these two intervals was < 1% and on the basis of this and other shipboard data, in particular results from a unique downhole logging programme, we believe that the clastic zone was first encountered at 310 m sub-bottom and was apparently continuous down to at least 405.5 m where the hole was abandoned.

Stratigraphic units within 396B were determined on the basis of macroscopic and microscopic lithologies, magnetic properties, chemical composition, alteration features and density of recovered samples. In addition, we have been able to correlate these units with downhole logging records which include sonic velocity, natural γ-ray intensity, porosity, density and electrical conductivity. Figure 1 summarises the general lithologies, magnetic inclination, chemical stratigraphy (typified by TiO_2 concentrations) and dual induction lateral (conductivity) log. All indicators show a marked change in character below the 310-m depth where samples of the clastic material were first recovered.

The gravel and sand from cores 30 and 33 are largely in the coarse sand to fine gravel size range (0.5–3.0 mm) and are moderately sorted. The sorting, however, may be the result of preferential loss of fine grained material during core recovery. The fragments are generally non-vesicular and consist of angular chips of glass and variolitic, cryptocrystalline and intersertal basalt. Olivine and plagioclase occur as phenocrysts in the clasts and as crystal fragments. A small number of pieces of calcite-cemented basaltic microbreccia, a few chips with calcite spherules and clasts with cross-cutting calcite veins were found. In general, the glass appears quite fresh, palogonite rims are uncommon and few palagonite fragments were found.

Two small fragments (5–10 cm) of bedded hyaloclastite were also recovered in core 30. One of these samples is a moderately indurated fine to coarse grained hyaloclastite sandstone with graded bedding and evidence for scouring. Both rocks offer clear evidence for some sort of current action and the redistribution of dominantly sand-sized fragments of sideromelane and fine grained basalt.

The last 90 m, which we have called the clastic zone, is divided into four units: an upper clastic breccia, an upper basaltic gravel, a plagioclase phyric pillow basalt (breccia?) and a lower gravel unit. The two gravel units seem to have been derived locally. Crystalline fragments in the upper gravel are